Self-consistent three-dimensional model of ultrashort terahertz pulse amplification in a laser-induced nonequilibrium plasma channel in xenon

© A.V. Bogatskaya [1,2], E.A. Volkova [3], A.M. Popov [1,2]

[1] Department of Physics, Moscow State University,
119991 Moscow, Russia
[2] Lebedev Physical Institute, Russian Academy of Sciences,
119991 Moscow, Russia
[3] Skobeltsyn Institute of Nuclear Physics, Moscow State University,
119991 Moscow, Russia

e-mail: annabogatskaya@gmail.com

The propagation and amplification of ultrashort terahertz pulses in a nonequilibrium photoionization plasma channel formed in xenon by a powerful femtosecond UV laser pulse is studied in three-dimensional geometry. The study is based on the self-consistent numerical integration of the second-order wave equation in cylindrical geometry and the Boltzmann kinetic equation in the two-term expansion to describe the electron velocity distribution function in the spatially inhomogeneous nonequilibrium plasma of the channel.

Keywords: nonlinear optics, terahertz radiation, nonequilibrium plasma channel, numerical simulation.

Introduction

A wide range of possible applications of terahertz radiation attracts great attention of specialists in various fields, such as molecular and solid state physics, spectroscopy, non-invasive diagnostics for medical purposes and security systems, quality control, wireless communication, remote sensing of the atmosphere, etc. [1–4].

In the present work, a complex self-consistent three-dimensional simulation of the process of amplification of high-power ultrashort terahertz (THz) pulses in nonequilibrium extended plasma channels formed in xenon during its multiphoton ionization by femtosecond UV laser pulses [5–9] is carried out. The calculations are based on joint integration of the second-order wave equation in cylindrical geometry and the system of Boltzmann kinetic equations for the velocity distribution function of electrons at different spatial points of the channel in a two-term approximation.

Model

Let's start the consideration with the second-order wave equation in cylindrical geometry (z axis is directed along the propagation of UV and THz pulses) for a linearly polarized short THz pulse propagating in a channel of nonequilibrium xenon plasma:

$$\frac{\partial^2 E}{\partial z^2} + \frac{1}{\rho}\frac{\partial}{\partial \rho}\left(\rho\frac{\partial E}{\partial \rho}\right) = \frac{1}{c^2}\frac{\partial^2 E}{\partial t^2} + \frac{4\pi}{c^2}\frac{\partial j}{\partial t}. \tag{1}$$

Here $\mathbf{r} = \{\rho, z\}$ is the radius vector, $E(\rho, z, t)$ is the electric field strength of the wave, $j(\rho, z, t)$ is current density in

plasma induced by THz pulse. The general approach for calculating such a current in a dispersive medium was considered in [10]. To analyze the pulse amplification process, as well as to determine its parameters, the wave equation (1) must be solved together with the system of Boltzmann kinetic equations to determine the electron velocity distribution function (EVDF) at various spatial points of the channel:

$$\frac{\partial f(\mathbf{r}, \mathbf{v}, t)}{\partial t} - \frac{e\mathbf{E}(\mathbf{r}, t)}{m}\frac{\partial f}{\partial \mathbf{v}} = St(f). \tag{2}$$

Here $f(\mathbf{r}, \mathbf{v}, t)$ — EVDF which is normalized according to the condition

$$\int f(\mathbf{r}, \mathbf{v}, t)d^3v = 1, \tag{3}$$

$\mathbf{E}(\mathbf{r}, t)$ — the electric field vector, and $St(f)$ is the collision integral, which generally takes into account both elastic and inelastic collisions of electrons.

If the drift velocity of electrons in an electric field is small compared to their thermal velocity, equation (2) can be analyzed within the two-term approximation [11,12]. Then

$$f(\mathbf{r}, \mathbf{v}, t) = f_0(\mathbf{r}, v, t) + \cos\vartheta f_1(\mathbf{r}, v, t) \tag{4}$$

(ϑ — the angle between the velocity vector and the electric field vector of the wave, where the zero harmonic $f_0(\mathbf{r}, v, t)$ determines the distribution of electrons over the absolute value of the velocity, and the first harmonic $f_1(\mathbf{r}, v, t)$ determines the asymmetry of the electron velocity distribution and makes it possible to find the electric current in the plasma:

$$j(\mathbf{r}, t) = -\frac{4\pi e N_e(\mathbf{r})}{3}\int v^3 f_1(\mathbf{r}, v, t)dv. \tag{5}$$

Here $N_e(\mathbf{r})$ is the electron concentration in the plasma. Substituting (4) into (2), we obtain a system of equations for the harmonics f_0 and f_1 at each spatial point of the channel [12]:

$$\frac{\partial f_0(\mathbf{r}, v, t)}{\partial t} = \frac{eE(\mathbf{r}, t)}{3mv^2} \frac{\partial}{\partial v} \left(v^2 f_1(\mathbf{r}, v, t) \right)$$

$$+ \frac{m}{M} \frac{1}{v^2} \frac{\partial}{\partial v} \left(\nu_{tr}(v) \left(v f_0 + \frac{T_g}{m} \frac{\partial f_0}{\partial v} \right) \right), \qquad (6)$$

$$\frac{\partial f_1(\mathbf{r}, v, t)}{\partial t} + \nu_{tr}(v) f_1(\mathbf{r}, v, t) = \frac{eE(\mathbf{r}, t)}{m} \frac{\partial f_0(\mathbf{r}, v, t)}{\partial v}. \qquad (7)$$

Here ν_{tr} — is the transport collision frequency, M is the xenon atom mass, $T_g = 0.025\,\text{eV}$ is the gas temperature.

In accordance with the model under consideration, a femtosecond UV laser pulse propagates in xenon along the z axis and creates a nonequilibrium plasma channel characterized by a Gaussian distribution of electron density along the radius and an isotropic EVDF with a spiked structure. For Xenon atoms (ionization potential $I_i \approx 12.13\,\text{eV}$) upon ionization by KrF laser radiation ($\hbar\Omega = 5.0\,\text{eV}$), the photoionization peak is characterized by the energy $\varepsilon_0 = 3\hbar\Omega - I_i \approx 2.87\,\text{eV}$. As was shown in [5], such a plasma is a medium for amplifying THz radiation. When simulating, we assume that the THz pulse propagates after the leading femtosecond UV pulse and is located in the amplification zone, which can be several centimeters [6–9]. We also believe that an ionizing femtosecond pulse propagates in a gas at the speed of light with almost no loss of energy, forming a channel with a uniform electron concentration along the z axis. The reference system is chosen so that the leading UV pulse is at the point $z = 0$.

Equation (1) was solved jointly with the system of equations for EVDF harmonics of zero and first orders (6), (7) at each node of the spatial grid. A brief discussion of the numerical procedure is contained in [9] and references cited in this works. Similarly [9] the integration time step was $\Delta t = 4 \cdot 10^{-15}\,\text{s}$, the spatial sampling step was $\Delta z = c\Delta t = 1.2 \cdot 10^{-4}\,\text{cm}$ and $\Delta\rho = 0.065\,\text{cm}$. The size of the counting region was chosen in the beam propagation direction (z axis) $L = 1.0\,\text{cm}$ and in the transverse direction $R_{\max} = 6.0\,\text{cm}$. The chosen integration time step made it possible to use an explicit scheme for the Boltzmann equation. The initial conditions for equations (1), (6) and (7) were chosen similarly [9].

Simulation results

First of all, let us dwell on the results of modeling the propagation of a weak THz seed pulse over a path length of $30\,\text{cm}$ in a nonequilibrium plasma channel in xenon with radii $R_0 = 0.5\,\text{cm}$ and $R_0 = 1.5\,\text{cm}$, radial profile $N_e = N_e^{(0)} \exp(-(\rho/R_0)^2)$ and different initial electron density $N_e^{(0)}$. The transverse size of the initial THz pulse was determined by the radius of the plasma channel $\rho_0 = R_0$.
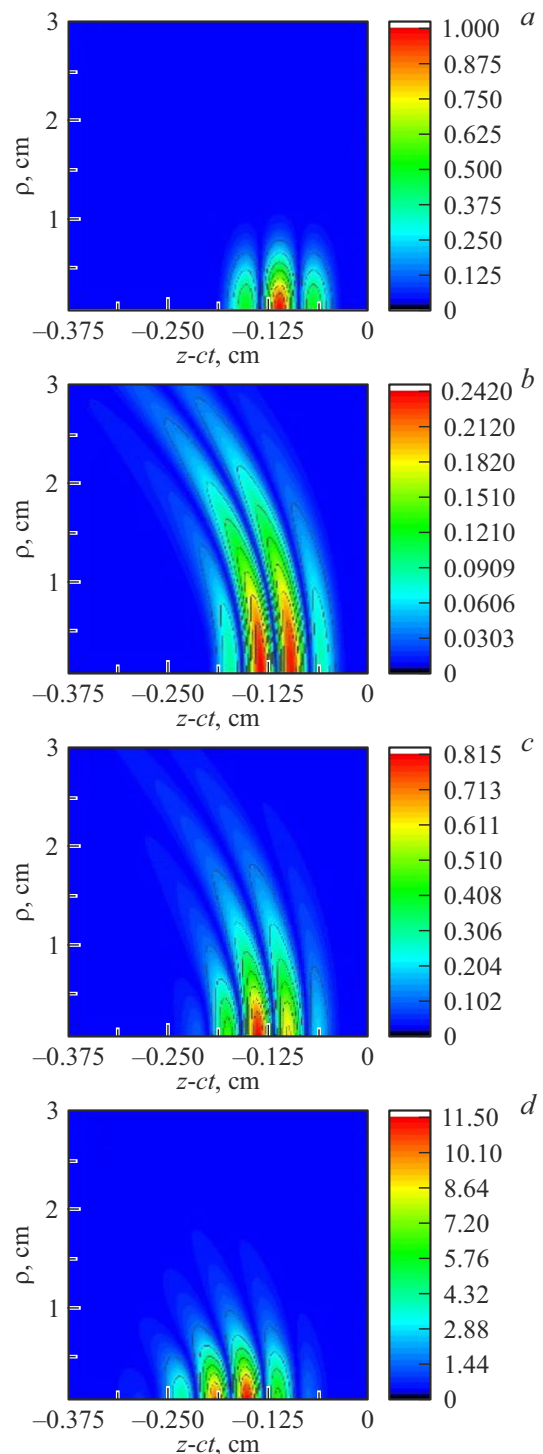
Figure 1. Spatial distribution of the absolute value of the electric field strength in a THz pulse: initial distribution (a), when propagating $30\,\text{cm}$ in free space (b), when propagating $30\,\text{cm}$ in a nonequilibrium plasma channel with gas density $10^{20}\,\text{cm}^{-3}$ with Gaussian electron density profile with values $N_e^{(0)} = 3 \cdot 10^{13}\,\text{cm}^{-3}$ (c) and $10^{14}\,\text{cm}^{-3}$ (d). The radial dimensions of the channel and the initial THz pulse are equal to $\rho_0 = R_0 = 0.5\,\text{cm}$. The level lines correspond to certain values of the electric field strength. The femtosecond UV pulse is located at $z - ct = 0$. Peak intensity of the initial pulse $1\,\text{W/cm}^2$.
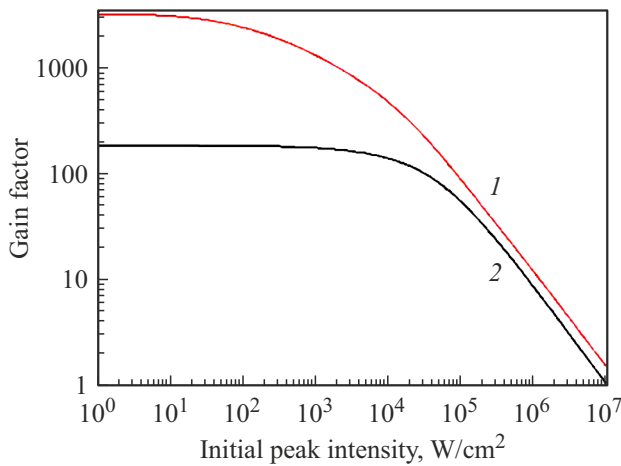
Figure 2. Gain factor (see (8)) depending on the peak intensity of the seed pulse for plasma channel radii $1.5\,\text{cm}$ (*1*) and $0.5\,\text{cm}$ (*2*).

The electron density distribution along the channel axis will be considered uniform.

Typical distributions of the spatial structure of the field for plasma electron densities 3×10^{13} and $10^{14}\,\text{cm}^{-3}$ and for gas density $N = 10^{20}\,\text{cm}^{-3}$, as well as for the case of pulse propagation in empty space, are shown in Fig. 1. The initial pulse is shown in Fig. 1, *a*. The data are normalized to the maximum value of the field strength in the seed pulse. First, in accordance with [6,7], we see that the plasma channel prevents diffusion spreading of the pulse in the radial direction: for a concentration of $10^{14}\,\text{cm}^{-3}$ the THz pulse is localized inside the plasma channel (Fig. 2, *d*), while for $N_e^{(0)} = 10^{13}\,\text{cm}^{-3}$ (Fig. 2, *c*) and especially for the case of propagation in free space (Fig. 2, *b*) diffraction divergence is noticeably more significant. These data confirm the statement made earlier [6] that the refraction index in a xenon plasma with a spiked EVDF structure can be greater than unity, i.e. such a plasma is an optically denser medium than a non-ionized gas. We also see that as the electron density increases, the time delay between the UV and THz pulses increases.

All previous calculations were related to relatively weak fields, which do not affect the evolution of the electron energy spectrum. To study the maximum possible pulse amplification in the channel and gain saturation, which is determined by the effect of the amplified pulse on the EVDF in the channel plasma, we calculated the gain dynamics for various values of the peak intensity of the initial pulse. For further data analysis, we introduced the amplification factor $g(L)$ as the ratio of the pulse energy over the length $L = 30\,\text{cm}$ to the initial one:

$$g(L) = \int E^2(\rho, z, t = L/c)\rho\, d\rho\, dz \Big/$$

$$\Big/ \int E^2(\rho, z, t = 0)\rho\, d\rho\, dz. \tag{8}$$
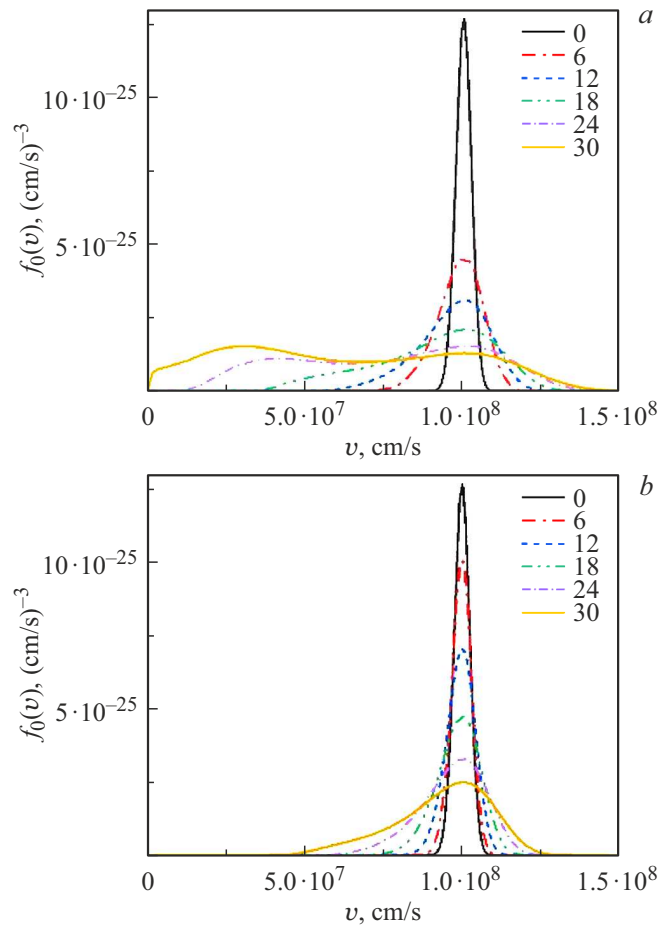
Figure 3. EVDF depending on the propagation length at the spatial point behind the leading UV pulse ($z - ct = -0.2\,\text{cm}$) for $\rho_0 = 0.5\,\text{cm}$, $I_0 = 10^5\,\text{W/cm}^2$. $N_e^{(0)} = 10^{14}\,\text{cm}^{-3}$, $N = 10^{20}\,\text{cm}^{-3}$. The radial coordinates are $\rho = 0$ (*a*) and $\rho = \rho_0$ (*b*). The propagation lengths (in cm) are given in the insert.

Calculation results for $N_e^{(0)} = 10^{14}\,\text{cm}^{-3}$, $N = 10^{20}\,\text{cm}^{-3}$ and two channel radii ($R_0 = 0.5\,\text{cm}$ and $R_0 = 1.5\,\text{cm}$) are shown in Fig. 2. As can be seen, the value of $g(L)$ is almost constant up to the intensity value $\leq 10^3\,\text{W/cm}^2$, and then rapidly decreases with increasing intensity. This decrease is the result of a significant rearrangement of the EVDF in the channel caused by the amplified pulse. Calculations show that, regardless of the initial radius of the plasma channel, the upper limit on the radiation intensity in a THz pulse is about $I^* \approx 10^7\,\text{W/cm}^2$.

For a more detailed understanding of the effect of saturation of the amplification of the THz pulse at the level $\sim 10^7\,\text{W/cm}^2$, Fig. 3 presents the results of calculating the evolution of the EVDF at the spatial point ($z - ct = -0.2\,\text{cm}$) behind the leading UV pulse both on the axis of the plasma channel ($\rho = 0$) and on its periphery ($\rho = \rho_0$).

As can be seen, in both cases, the amplified THz signal causes a strong rearrangement of the EVDF, destroying the peak structure of the spectrum created by the UV pulse. As
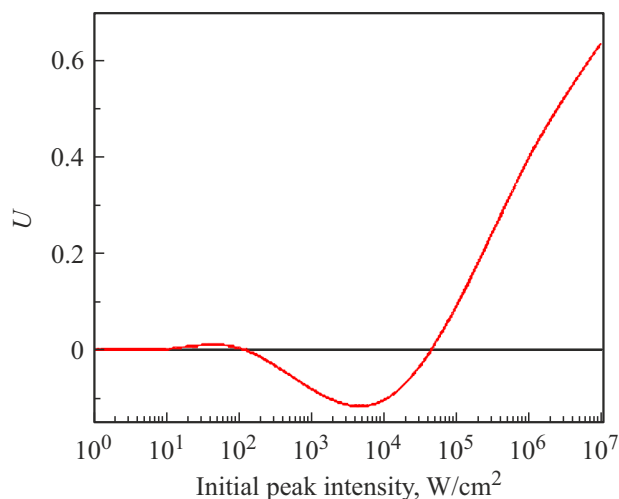
Figure 4. The degree of pulse unipolarity depending on the peak value of the intensity of the initial pulse at a propagation length of 30 cm in a plasma channel in xenon with parameters $R_0 = 1.5$ cm, $N_e^{(0)} = 10^{14}$ cm^{-3}, $N = 10^{20}$ cm^{-3}.

a result, the enhancement in plasma decreases with time and then gives way to absorption. In this case, the most rapid rearrangement of the EVDF occurs on the channel axis in the region of a strong field. As a result, both the radial and z axis field distributions can be significantly distorted. In this case, the calculations show a possible shortening of the initial pulse length and the formation of unipolar THz pulses [13–17]. The degree of unipolarity (U-factor) of such pulses can be conveniently characterized quantitatively by the normalized „area" of the pulse, defined as

$$U = \frac{\int E(\rho, z)\rho d\rho dz}{\int |E(\rho, z)|\rho d\rho dz}. \qquad (9)$$

A typical dependence of the degree of pulse unipolarity, calculated using (9) for a pulse path length of 30 cm in the channel plasma, for various values of its initial peak intensity is shown in Fig. 4. Note that the sign of the U factor changes depending on the intensity of the initial pulse due to the emerging spatial inhomogeneity of its amplification as it moves in the plasma channel. Calculations have shown that a significant degree of unipolarity arises only at initial intensities exceeding 10^6 W/cm^2, when a significant distortion of the EVDF leads to the fact that only the leading edge of the seed pulse is in the amplification zone.

Conclusion

Thus, in this paper, a model for the propagation and amplification of THz pulses in a nonequilibrium plasma channel in xenon is constructed. The model is based on the numerical integration of a three-dimensional second-order wave equation in cylindrical geometry for the THz pulse field together with the Boltzmann kinetic equation describing the evolution of the electron velocity distribution

function at various spatial points of the plasma channel. It is shown that the nonequilibrium plasma of the channel formed upon ionization of xenon by a KrF laser pulse is not only an amplifying but also a focusing medium, which makes it possible to use such a plasma as an independent waveguide for efficient transport of THz pulses. In relatively weak fields (initial radiation intensity in the channel $\leq 10^3$ W/cm^2), the reverse effect of the amplified pulse on the evolution of the electron velocity distribution can be neglected. However, when the intensity reaches $\sim 10^5 - 10^6$ W/cm^2, the propagating THz pulse destroys the spike structure of the electron spectrum, which leads to a decrease and then to the disappearance of the gain in the channel and, simultaneously, to an increase in the radius of the THz beam. As a result, a shortening of the THz pulse duration is observed. In particular, it becomes possible to form unipolar THz pulses that have a unidirectional effect of radiation on matter.

Conflict of interest

The authors declare that they have no conflict of interest.

References

[1] B. Fischer, M. Walther, P. Jepsen. Phys. Med. Biol., **47**, 3807 (2002). DOI: 10.1088/0031-9155/47/21/319

[2] M. Tonouchi. Nat. Photon., **1**, 97 (2007). DOI: 10.1038/nphoton.2007.3

[3] S. Fleischer, Y. Zhou, R.W. Field, K.A. Nelson. Phys. Rev. Lett., **107**, 163603 (2011). DOI: 10.1103/PhysRevLett.107.163603

[4] T. Kampfrath, K. Tanaka, K. Nelson. Nature Photon., **7**, 680 (2013). DOI: 10.1038/NPHOTON.2013.184

[5] A.V. Bogatskaya, A.M. Popov. JETP Lett., **97**(7), 388 (2013). DOI: 10.1134/S0021364013070035

[6] A.V. Bogatskaya, I.V. Smetanin, E.A. Volkova, A.M. Popov. Las. Part. Beams, **33**(1), 17 (2015). DOI: 10.1017/S0263034614000755

[7] A.V. Bogatskaya, Hou Bin, I.V. Smetanin, A.M. Popov. Phys. Plasmas, **23**(9), 093510 (2016). DOI: 10.1063/1.4962515

[8] A.V. Bogatskaya, N.E. Gnezdovskaia, A.M. Popov. Phys. Rev. E., **102**(4), 043202 (2020). DOI: 10.1103/PhysRevE.102.043202

[9] A. V. Bogatskaya, E.A. Volkova, A.M. Popov. J. Opt. Soc. Am. B, **39**(1), 299 (2022). DOI: 10.1364/JOSAB.435710

[10] A.V. Bogatskaya, A.M. Popov. Las. Phys. Lett., **16**(6), 066008 (2019). DOI: 10.1088/1612-202X/ab183d

[11] V.L. Ginzburg, A.V. Gurevich. Sov. Phys. Usp., **3**(1), 115 (1960). DOI: 10.1070/PU1960v003n01ABEH003261

[12] Yu.P. Raizer. *Lazernaya iskra i rasprostraneniye razryadov* (Nauka, M., 1974) (in Russian)

[13] A.V. Pakhomov, R.M. Arkhipov, I.V. Babushkin, M.V. Arkhipov, Yu.A. Tolmachev, N.N. Rosanov. Phys. Rev. A., **95**, 013804 (2017). DOI: 10.1103/PhysRevA.95.013804

[14] R.M. Arkhipov, A.V. Pakhomov, M.V. Arkhipov, A. Demircan, U. Morgner, N.N. Rosanov, I. Babushkin. Phys. Rev. A., **101**, 043838 (2020). DOI: 10.1103/PhysRevA.101.043838

[15] R. Arkhipov, M. Arkhipov, A. Pakhomov, I. Babushkin, N. Rosanov. Las. Phys. Lett., **19**(4) 043001 (2022). DOI: 10.1088/1612-202X/ac5522

[16] A.V. Bogatskaya, E.A. Volkova, A.M. Popov. Phys. Rev. E., **104**, 025202 (2021). DOI: 10.1103/PhysRevE.104.025202

[17] A.V. Bogatskaya, E.A. Volkova, A.M. Popov. Plasma Sour. Sci. Technol., **30**(8), 085001 (2021). DOI: 10.1088/1361-6595/ac0a4b